

# Substrate Material Optimization for Bowtie Antenna for High Frequency Applications

Parveen Kour, Harish Kumar, Saleem Khan

**Abstract**— The research work is carried out to optimize the substrate material of high frequency antenna design and simulation. Three different high-k substrate materials were consider for the design process. 2mm thick arlon, roger, and Al<sub>2</sub>O<sub>3</sub> material were taken as the substrate for the bowties antenna. The designed antenna were analysed in frequency domain in the range of 26 GHz to 40 GHz. S-parameter and directivity were analysed for Ka band application.

**Index Terms**— s-parameters, Ka band, high-k, narrow band

## I. INTRODUCTION

Now-a-day all communication systems in government and commercial sectors have been to develop a small, lightweight, low profile and cost effective antennas that are capable of keeping high performance over a wide range of frequencies. The main focus of this developed technology is into the design of microstrip patch antennas. Microstrip patch antennas exhibit many advantages than other antennas with simple structure. They are very light weight, simple, low profile and cost effective to fabricate using printed circuit board technology and also they are conformal to planar and non-planar surfaces [1-2].

Microstrip patch antennas have a number of disadvantages too. Some of their main drawbacks are the low gain, narrow bandwidth and surface wave excitation that reduce radiation efficiency. To overcome narrow bandwidth different methods have been used [3]. A ferrite composition and a thick substrate whose dielectric constant is low provide a wide bandwidth but the first approach leads to no low-profile designs, whereas the second solution is expensive. The fabrication process is difficult of this technique. The bandwidth of the antenna may be improved by using the proximity/aperture coupled feeding methods. Bandwidth is also enhanced by using the stack multi-resonator configuration but it has a large thickness prototype [4,5]. The surface waves of the antenna have been decrease by using the electromagnetic band-gap. An array of patch elements is used to obtain a high gain antenna. From advantages of the Microstrip patch antennas the aim of the researchers is to overcome their de-merits to benefit [6-9]. The applications are in the various fields such as in the medical applications, satellites and of course even in the body worn antenna for military personal and military systems just like in the rockets, mobile systems, broadcast radio, television, vehicle collision avoidance system, satellite communications, surveillance systems, radar systems and remote sensing, aircrafts missiles, global positioning system (GPS), radio-frequency identification (RFID) [6] etc. Now they are burgeoning for the cost effective fabrication techniques in the commercial aspects. Due to the increasing usage of the patch antennas in

the wide range, it is also expected that this could take over the usage of the usual antennas for the maximum applications [10-12].

The design of basic microstrip patch antenna consists of metallic patch and metallic ground plane that are printed on other sides of the dielectric substrate. Thickness of radiating plane and ground plane are  $t \ll \lambda_0$  where,  $t$  is the thickness of the metal layers and  $\lambda_0$  is the free space resonant wavelength of the microstrip antenna. Thickness of dielectric substrate is  $h \ll \lambda_0$ , usually  $0.003 \lambda_0 \leq h \leq 0.05 \lambda_0$ . Length  $L$  of the patch is usually  $0.3333 \lambda_0 < L < 0.5 \lambda_0$ . Relative permittivity of the substrate is usually  $2.2 \leq \epsilon_r \leq 12$ . The radiation characteristic of the MPA depends on the fringing field which increases with increasing substrate height and decreasing the relative permittivity of the substrate. The metallic patch is normally etched using a photolithographic process. The metallic patch normally made of copper or gold may take virtually any shape, but for simplification of the analysis and performance prediction regular shapes are commonly used [13-15].

In this research paper material optimization for bowtie antenna working in Ka band is carried out. Frequency domain analysis is done for the frequency range of 26 GHz to 40 GHz.

## II. SIMULATION PROCESS FLOW

Simulation of Ka band microstrip patch antenna in HFSS is carried out in following steps: creating geometry, assigning material to the geometry, validating the simulation, and analyzing the structure in frequency domain. Substrate is created using e a box with coordinates X: -17.0, Y: -32, Z: 0.0 and dimensions of dX: 34.0, dY: 64.0, dZ: -2.0.

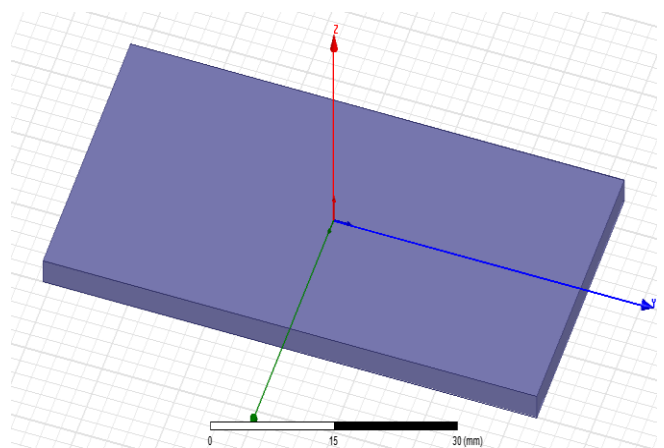


Fig. 1 Substrate for antenna design.

Creating perfect electric conductor layer (PEC): Draw a rectangle with coordinates X: -17.0, Y: -32.0, Z: 0.0 and dimensions dX: 34.0, dY: 64.0, dZ: 0.0.

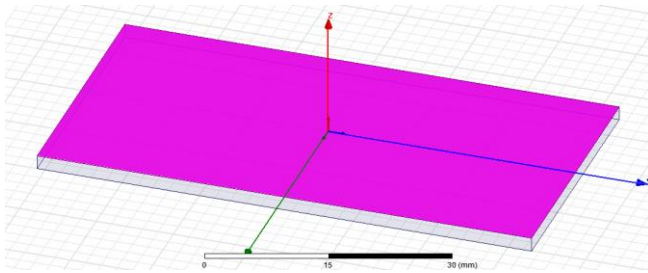


Fig. 2 PEC layer for patch design.

After creating the PEC layer structure of the antenna is created using polyline and rectangle, which is subtracted from the PEC layer leaving only the structure above the substrate. Finally the box is created to emulate the radiation patterns of the antenna.

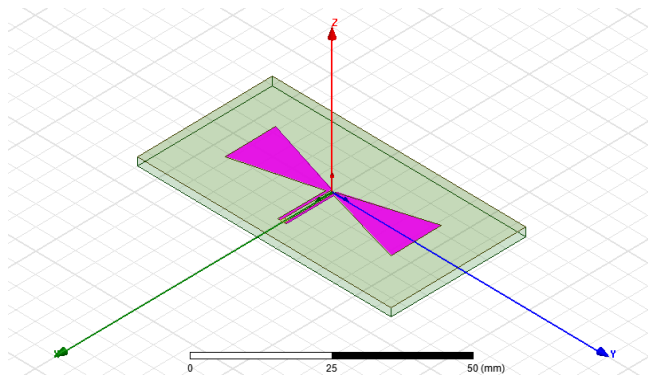


Fig. 3 Designed antenna for Ka band.

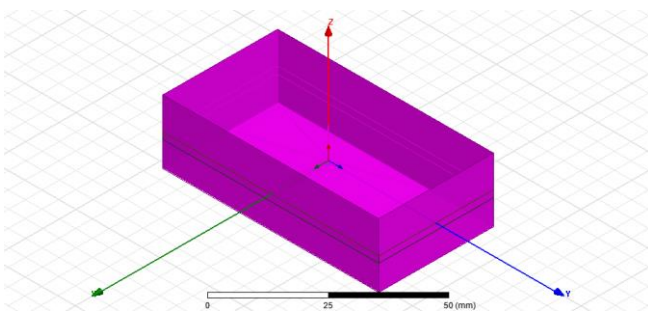


Fig. 4 Infinite sphere box for boundary conditions.

Boundary conditions specify the field behavior at the edges of the problem region and object interfaces.

You may assign the following types of boundaries to an design:

- Perfect E: Represents a perfectly conducting surface.
- Perfect H: Represents a surface on which the tangential component of the H-field is the same on both sides.
- Impedance: Represents a resistive surface.
- Radiation: Represents an open boundary by means of an absorbing boundary condition (ABC) that absorbs outgoing waves.
- PML: Represents an open boundary condition using several layers of specialized materials that absorb outgoing waves.
- Finite Conductivity: Represents an imperfect conductor.
- Symmetry: Represents a perfect E or perfect H plane of symmetry.
- Master: Represents a surface on which the E-field at each point is matched to another surface (the slave boundary) to within a phase difference.
- Slave: Represents a surface on which the E-field at each

point has been forced to match the E-field of another surface (the master boundary) to within a phase difference.

- Lumped RLC: Represents any combination of lumped resistor, inductor, and/or capacitor in parallel on a surface.
- Anisotropic Impedance: Represents a boundary condition used to replace a surface a planar screen or grid with periodic geometry.
- Layered Impedance: Represents a structure with multiple layers as one impedance surface.
- IE Region: Represents a conductor or dielectric that you assign to be solved using the IE solver.

Excitations are sources of electromagnetic fields in the design. HFSS has various options to generate incident fields that interact with a structure to produce the total fields. Some of these excitations are local sources residing within the structure such as lumped port and voltage sources, while other excitations such as plane waves are created from local sources away from the structure.

HFSS generates an initial mesh, which includes surface approximation settings. If necessary, the mesher will automatically perform any repairs needed to recover an accurate mesh representation of a model. The solution profile will indicate when mesh repairs have been made, and the results of these repairs will be displayed per object in the mesh statistics panel. If lambda refinement was requested, it refines the initial mesh based on the material-dependent wavelength.

## III. RESULTS AND DISCUSSION

A conventional bowtie patch antenna is designed and simulated for Ka band i.e. frequency range from 26 GHz to 40 GHz. Lumped feeding technique is used for excitation as discussed in methodology section. In order to optimize the performance of the antenna three different substrate materials were chosen. The material properties are given in Table 1.

After simulation process is completed, S-parameter and 3-D polar plot of directivity shown in Fig. 5 and Fig. 6 respectively. The resonant frequency of the designed antenna is approximately 33.80 GHz and the insertion loss is -13.75 dB. Directivity 3D plot describes the radiation pattern of the antenna. Insertion loss for frequency ranging from 26 GHz to 40 GHz with 1 GHz is tabulated in Table 2.

Table 5.1 Substrate material properties

| Properties              | Roger RO3010 (tm) | Arlon AD270 (tm) | Al2O3       |
|-------------------------|-------------------|------------------|-------------|
| Relative Permittivity   | 10.2              | 2.7              | 9.8         |
| Relative Permeability   | 1                 | 1                | 1           |
| Bulk Conductivity       | 0 siemens/m       | 0 siemens/m      | 0 siemens/m |
| Magnetic Saturation     | 0 tesla           | 0 tesla          | 0 tesla     |
| Dielectric Loss Tangent | 0.0035            | 0.0023           | 0           |
| Relative Permittivity   | 10.2              | 2.7              | 9.8         |
| Relative Permeability   | 1                 | 1                | 1           |

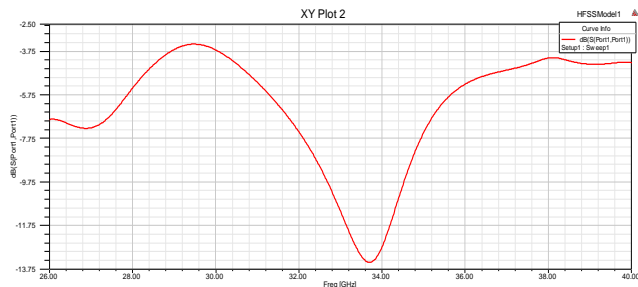


Fig. 5 Insertion loss of designed antenna with arlon substrate.

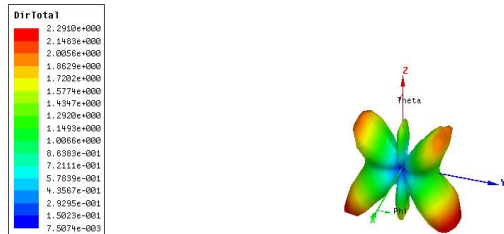


Fig. 6 3D directivity polar plot for antenna with arlon substrate.

Table 2 Insertion loss for arlon substrate with conventional design.

| Frequency (GHz) | Insertion Losses (dB) |
|-----------------|-----------------------|
| 26              | -6.88201              |
| 27              | -7.26098              |
| 28              | -5.45043              |
| 29              | -3.67708              |
| 30              | -3.69596              |
| 31              | -5.18091              |
| 32              | -7.44543              |
| 33              | -11.0807              |
| 34              | -12.709               |
| 35              | -7.48241              |
| 36              | -5.25892              |
| 37              | -4.61761              |
| 38              | -4.06356              |
| 39              | -4.34862              |
| 40              | -4.28543              |

Figure 7 shows S-parameter for frequency ranging from 26 GHz to 40 GHz. With roger substrate the designed antenna shows three resonant frequencies 32.20 GHz, 33.40 GHz, and 36.40 GHz with insertion losses -13.70 dB, -12.50 dB, and -12.80 dB respectively. Figure 8 shows the 3D directivity polar plot of the designed conventional antenna. Insertion loss for frequency ranging from 26 GHz to 40 GHz having step size of 1 GHz with roger substrate is tabulated in Table 3.

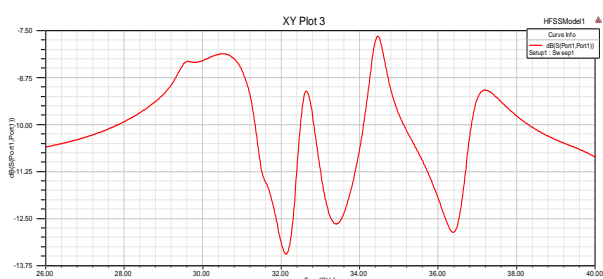


Fig. 7 Insertion loss of designed antenna with roger substrate.



Fig. 8 3D directivity polar plot for antenna with roger substrate.

Table 3 Insertion loss for roger substrate with conventional design.

| Frequency (GHz) | Insertion Losses (dB) |
|-----------------|-----------------------|
| 26              | -10.5955745           |
| 27              | -10.3386317           |
| 28              | -9.923360783          |
| 29              | -9.19860021           |
| 30              | -8.302604673          |
| 31              | -8.555808231          |
| 32              | -13.12332385          |
| 33              | -11.22834771          |
| 34              | -10.63772783          |
| 35              | -9.730281657          |
| 36              | -11.95884939          |
| 37              | -9.299158853          |
| 38              | -9.771498413          |
| 39              | -10.40310517          |
| 40              | -10.86262917          |

Figure 9 shows S-parameter for frequency ranging from 26 GHz to 40 GHz. With Al<sub>2</sub>O<sub>3</sub> substrate the designed antenna shows three resonant frequencies 32.80 GHz and 34.20 GHz with insertion losses -13.50 dB and -14.20 dB respectively. Figure 10 shows the 3D directivity polar plot of the designed conventional antenna. Insertion loss for frequency ranging from 26 GHz to 40 GHz having step size of 1 GHz with roger substrate is tabulated in Table 4.

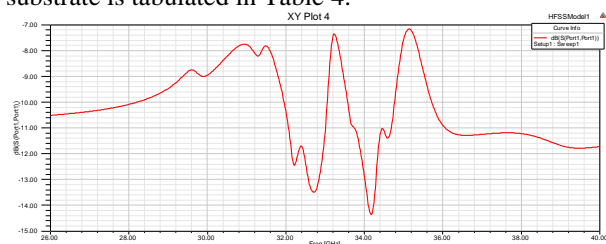


Fig. 9 Insertion loss of designed antenna with Al<sub>2</sub>O<sub>3</sub> substrate.



Fig. 10 3D directivity polar plot for antenna with Al<sub>2</sub>O<sub>3</sub> substrate.

Table 4 Insertion loss for roger substrate with conventional design.

| Frequency (GHz) | Insertion Losses (dB) |
|-----------------|-----------------------|
| 26              | -10.50791404          |
| 27              | -10.35435525          |
| 28              | -10.08254771          |
| 29              | -9.469473702          |
| 30              | -8.955160214          |
| 31              | -7.769570355          |
| 32              | -10.35512069          |
| 33              | -11.10793577          |
| 34              | -12.87651603          |
| 35              | -7.564690486          |
| 36              | -10.89772972          |
| 37              | -11.23962746          |
| 38              | -11.21213244          |
| 39              | -11.67130526          |
| 40              | -11.71129113          |

## IV. CONCLUSION

The research work conventional bowtie antenna is designed and simulated for frequency ranging from 26 GHz and 40 GHz. Three different substrate material arlon, roger, and Al<sub>2</sub>O<sub>3</sub> were used for the patch antenna. It is observed from the results that single resonant frequency is observed for arlon substrate, triple resonant frequency were observed for roger substrate, and double resonant frequency were observed for Al<sub>2</sub>O<sub>3</sub> substrate.

## REFERENCES

- [1] Newman, E.H. and Tylyathan, P., "Analysis of Microstrip Antennas Using Moment Methods," IEEE Trans. Antennas Propag., Vol. AP-29, No. 1, pp. 47-53, January 1981.
- [2] C. Fritzsche, S. Bildik, and R. Jakoby, "Ka-band frequency tunable patch antenna," Proceedings of the 2012 IEEE International Symposium on Antennas and Propagation, Jul. 2012.
- [3] S. Zhao and D. R. Chen, "Design of Ka-Band Conformal Microstrip Patch Antenna," Advanced Materials Research, vol. 1046, pp. 289-292, Oct. 2014.
- [4] Z. L. Deng and H. Moran, "Design and Simulation of a Ka-Band Pattern Reconfigurable Microstrip Patch Antenna," Advanced Materials Research, vol. 875-877, pp. 1170-1175, Feb. 2014.
- [5] A. K. Patel, K. Jaiswal, A. K. Pandey, S. Yadav, K. Srivastava, and R. Singh, "A Compact Inverted V-Shaped Slotted Triple and Wideband Patch Antenna for Ku, K, and Ka Band Applications," Recent Trends in Communication, Computing, and Electronics, pp. 59-67, Dec. 2018.
- [6] D. Liu, X. Gu, C. W. Baks, and A. Valdes-Garcia, "Antenna-in-Package Design Considerations for Ka-Band 5G Communication Applications," IEEE Transactions on Antennas and Propagation, vol. 65, no. 12, pp. 6372-6379, Dec. 2017.
- [7] W.-C. Liao, R. Maaskant, T. Emanuelsson, M. Johansson, A. Hook, J. Wettergren, M. Dieudonne, and M. Ivashina, "A Ka-Band Active Integrated Antenna for 5G Applications: Initial Design Flow," 2018 2nd URSI Atlantic Radio Science Meeting (AT-RASC), May 2018.
- [8] Ramesh Garg, Prakash Bartia, Inder Bahl and Apisak Ittipiboon, "Microstrip Antenna Design Handbook", Artech House Inc. Norwood, MA., Pp.1-68, 2001.
- [9] 6. Wentworth M. Stuarts, "Fundamentals of electromagnetics with Engineering Applications", John Wiley & Sons, NJ, USA, Pp.442-445, 2005.
- [10] Deschamps and G.A., "Microstrip Microwave Antennas", 3rd USAF Symposium on Antennas, 1953.
- [11] Gutton, H. and G. Baissinr, "Flat Aerial for Ultra High Frequencies", French patent No. 70313, 1955.

- [12] Howell, J.Q., "Microstrip Antennas", Tee AP-S Int. Symp. Digest, 1972.
- [13] Munson and R.E., "Conformal Microstrip Antennas and Microstrip Phased arrays", IEEE Transaction on Antennas and Propagation, Vol.22, Pp.74-78, 1974.
- [14] R.J. Mailloux, J.F. Mellvanna and N.P Kernweis, "Microstrip Array Technology", IEEE Transaction on
- [15] Antennas and Propagation, Vol.29, Pp-25-37, 1981. J.M.Jin and J.L.Volakis, "A Hybrid Finite Element Method for Scattering and Radiation by Microstrip Patch Antennas and Arrays Residing in a Cavity", IEEE Transaction on Antennas and Propagation, Vol.-39, Pp-25-37, 1991